Cellular Response to Gelatin- and Fibronectin-Coated Multilayer Polyelectrolyte Nanofilms

Mengyan Li, David K. Mills, Tianhong Cui, and Michael J. McShane*, *Member, IEEE*

***Abstract*—Surface engineering is a critical effort in defining substrates for cell culture and tissue engineering. In this context, multilayer self-assembly is an attractive method for creating novel composites with specialized chemical and physical properties that is currently drawing attention for potential application in this area. In this work, effects of thickness, surface roughness, and surface material of multilayer polymer nanofilms on the growth of rat aortic smooth muscle cells were studied. Polyelectrolyte multilayers (PEMs) electrostatically constructed from poly(allylamine hydrochloride) and poly(sodium 4-styrenesulfonate) (PSS) with gelatin, fibronectin, and PSS surface coatings were evaluated for interactions with smooth muscle cells (SMCs) in an *in vitro* environment. The results prove that PEMs terminated with cell-adhesive proteins promote the attachment and further growth of SMCs, and that this property is dependent upon the number of layers in the underlying multilayer film architecture. Cell roundness and number of pseudopodia were also influenced by the number of layers in the nanofilms. These findings are significant in that they demonstrate that both surface coatings and underlying architecture of nanofilms affect the morphology and growth of SMCs, which means additional degrees of freedom are available for design of biomaterials. This work supports the excellent potential of nanoassembled ultrathin films for biosurface engineering, and points to a novel perspective for controlling cell–material interaction that can lead to an elegant system for defining the extracellular *in vitro* environment.**

***Index Terms*—Fibronectin (FN), gelatin, layer-by-layer (LbL) self-assembly, nanofilms, polyelectrolyte multilayers (PEMs), smooth muscle cells (SMCs).**

I. Introduction

THE interaction of cells with their extracellular matrix (ECM) generates a complex series of signaling events which serve to regulate several aspects of cell behavior, including adhesion, proliferation, differentiation, and motility [1]–[5]. Tuning the interactions of cells to the engineered matrix is a major challenge in tissue engineering. In recent years, it has become evident that surface chemical properties of the engineered scaffolds are the primary factors in determining cell behavior for *in vitro* cultures [6]–[9].

Electrostatic layer-by-layer (LbL) self-assembly has recently been employed in the fabrication of ultrathin films from charged polyions (polymers), dyes, nanoparticles, proteins, and other supramolecular species [10]–[17]. The main idea of this method consists in the resaturation of polyion adsorption, which results in the alternation of the terminal charge after each layer is deposited, allowing precise manufacture of polyelectrolyte multilayers (PEMs). With this approach, surface modification procedures have been developed to control cell–material interactions based on the exposed chemical moieties [18]–[20].

Proteins such as collagen, fibronectin (FN), or peptides containing integrin-binding domains have often been used to increase the attachment of specific cells for a designed substrate in an *in vitro* environment [21]–[26]. *In vivo*, collagen acts as scaffolding for human bodies and controls cell shape and differentiation while gelatin, essentially denatured collagen isolated from animal skin and bones, is inexpensive and widely used in many scientific and industrial applications [9], [27], [28]. The ECM also contains noncollagenous adhesive proteins, such as FN or vitronectin, which play critical roles in organizing the matrix and in enabling cells to attach to it [29], [30].

In previous studies using LbL assembly for surface modification, gelatin- and FN-terminated nanofilms were both found to promote cell attachment and growth [9], [23], [25]. However, an interesting difference in the cell adhesion process was observed using substrates patterned with protein on a background of polycation poly(diallyldimethyl ammonium chloride) (PDDA): in a direct comparison, smooth muscle cells (SMCs) initially attached to gelatin-coated regions rather than PDDA-coated areas, while the cells presented with FN patterns initially attached to PDDA and then migrated to FN regions [31]. Furthermore, it has been shown that FN assembles differently onto poly(sodium 4-styrenesulfonate) (PSS)- and poly(allylamine hydrochloride) (PAH)-terminated films, resulting in altered physicochemical properties at the substrate surface, which translate directly into changed cell adhesion behavior due to the varying accessibility of the integrin-binding region of the protein [32]. While it is generally understood that the material of the outmost layer, which interacts with the cells growing on it, is the major mediating factor in determining the surface properties of these substrates, some evidence suggests that underlying material properties may play a significant role in determining cell adhesion. Furthermore, it has been demonstrated that the molecular architecture of the ultrathin polymer films may direct a particular multilayer combination to be either cell adhesive or cell resistant, and this may be changed dynamically through pH or other factors [19].

In this paper, PEM nanofilms assembled from polymers and proteins were investigated for cell–matrix interactions *in vitro*. Specifically, the dependence of cell adhesion and morphology on terminal layer chemistry, structure, and underlying film thickness were studied. FN, gelatin, and PSS-coated

Manuscript received July 13, 2004; revised August 26, 2004. This work was supported by the National Science Foundation under Grant 0092001). Any opinions, findings, and conclusions or recommendations expressed in this material are those of the authors and do not necessarily reflect the view of the National Science Foundation. *Asterisk indicates corresponding author.*

M. Li, D. K. Mills, and T. Cui are with the Institute for Micromanufacturing, Ruston, LA 71272.

*M. J. McShane is with the Institute for Micromanufacturing, Ruston, LA 71272 (e-mail: mcshane@latech.edu).

Digital Object Identifier 10.1109/TNB.2005.850477

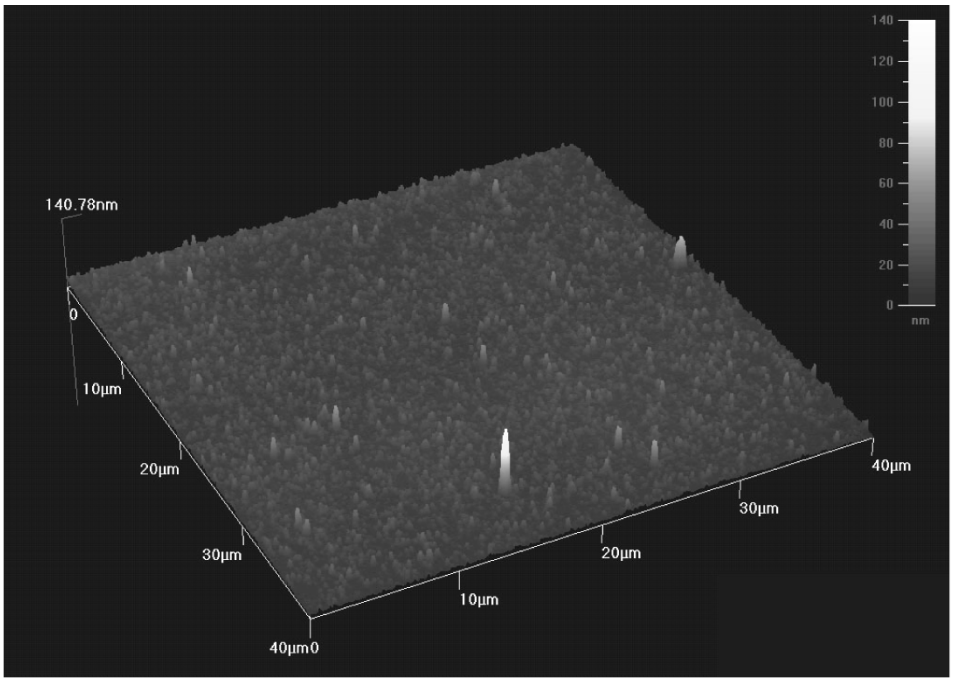

Fig. 1. AFM image of $(PAH/PSS)_{10}$ nanofilms deposited on a glass substrate.

surfaces with 1-, 2-, 5-, 10-, and 20-bilayer PAH/PSS underlying architectures on glass substrates were fabricated using the LbL process. The films were characterized using atomic force microscopy (AFM), and the influence of the multilayer assemblies on cell response was then investigated using rat aortic SMCs (RASMCs), for which the cell shape, cytoskeletal arrangement, and formation of focal adhesions were used to compare substrates and identify relationships between cell response and scaffold composition, thickness, and structure. This study is a part of several studies aimed at deeper understanding of cell–material interactions, which will allow for improved design and production of biomaterials to elicit specific cellular responses.

II. Materials and Methods

A. Materials and Instrumentation

PAH (polycationic, MW 15 000), PDDA (polycationic, MW 400 000-500 000), and PSS (polyanionic, MW 70 000) from Sigma-Aldrich, St. Louis, MO, were used as charged polymers. Gelatin (Bloom 225, Type B, Sigma-Aldrich) and FN (Sigma Chemical Co.) were used for cell-adhesive surface coatings. Polyelectrolyte and protein solutions for adsorption were 2 mg/mL with 0.5 M KCl in deionized (DI) water at pH 5.5, and the adsorption experiments were performed at the same pH except as otherwise specified. Nano-Strip was purchased from Cyantek Corporation. Glass substrates were standard microscope slides from Fisher.

All cells used were RASMCs, generously donated by Louisiana State University Health Sciences Center, Shreveport. RPMI-1640 cell culture medium (HyQ RPMI-1640 medium cell culture reagents, HyClone) supplemented with 5%–10% fetal bovine serum (FBS, Atlanta Biologicals) was used as basic nutrition for SMCs. A Vybrant Apoptosis Assay Kit #5 (Hoechst 33 342/propidium iodide) and phalloidin labeled with Alexa Fluor 488 were purchased from Molecular Probes to stain nuclei and F-actin.

TABLE I
Roughness of (PAH/PSS) Multilayer Nanofilms

# of Bilayers	Nanofilm Architecture	Roughness (nm)	
		Average	S.D.
2	$(PAH/PSS)_2$	9.64	1.69
5	$(PAH/PSS)_5$	11.21	0.58
10	$(PAH/PSS)_{10}$	13.21	0.73
20	$(PAH/PSS)_{20}$	20.31	3.01

Characterization of the multilayer films was performed with an AFM (Q-Scope 350, Quesant Instrument Corp.). Cells were observed and imaged with an inverted epifluorescence microscope (Nikon Eclipse TS100) equipped with a Nikon CoolPix 995 camera. Images were collected separately for the different chromophores (UV excitation with DAPI cube, blue excitation with FITC cube), and images were overlaid using Adobe Photoshop.

B. Experimental Procedures

1) Fabrication of Polyelectrolyte Nanofilms: The deposition of nanocomposite polyelectrolyte films was achieved using electrostatic LbL self-assembly. The standard layering process was as follows: individual aqueous solutions of polyion and protein at concentration of 2 mg/mL were prepared and adjusted to the appropriate pH. For each case, the substrate was prepared by incubation in Nanostrip solution at 70 °C for one hour to remove organic contaminants and induce a negatively charged surface such that the initial electrostatic coating step would be readily started. The substrate was then alternately immersed in polyion solutions for 10 min or protein solutions

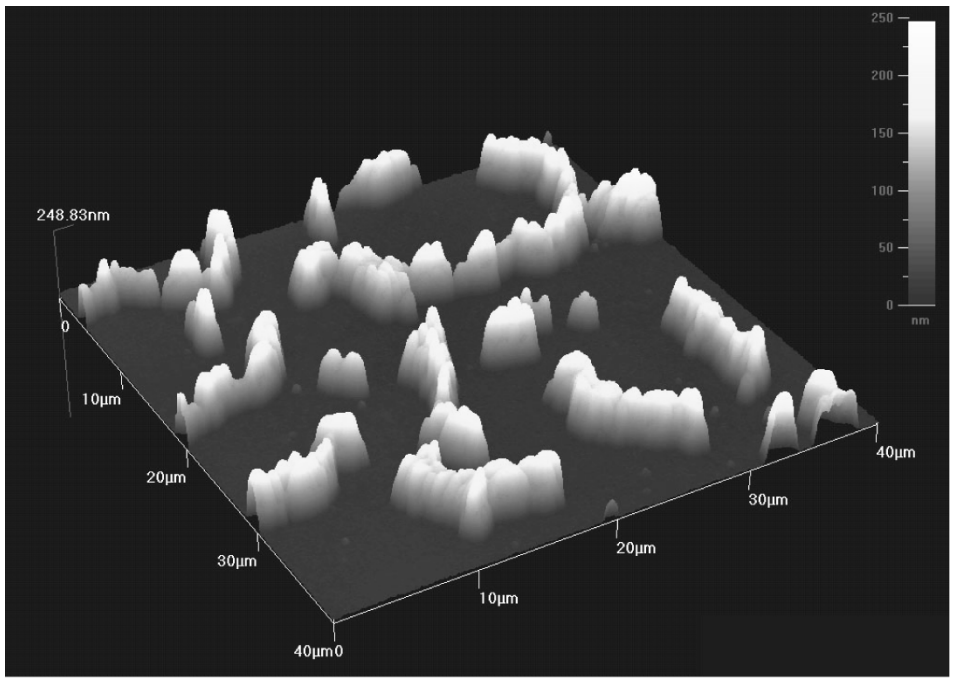

Fig. 2. AFM image of gelatin-terminated nanofilm $\{(\text{PAH/PSS})_{20}/\text{PAH}/\text{gelatin}\}$ deposited on a glass substrate.

for 20 min, respectively, with intermediate triple rinses with DI water in all cases.

2) Characterization of Polyelectrolyte Nanofilms: Multilayer polyelectrolyte ultrathin films of varying thickness—denoted as $(\text{PAH/PSS})_n$ where $n = 1, 2, 5, 10,$ or 20—were deposited on the planar glass substrates with the standard LbL self-assembly procedure. Gelatin or FN was then deposited on the surface of the polyelectrolyte films, as appropriate for the experiment. The overall architecture of the sampled prepared with polyelectrolyte thin films include the following: 1) $(\text{PAH/PSS})_n$; 2) $(\text{PAH/PSS})_n$ + FN; and 3) $(\text{PAH/PSS})_n$ + PAH/gelatin. These nanofilms were used to study the effect of surface materials and underlying architectures on cell adhesion and growth. By using AFM, the surface topology of molecular/cluster structures may be profiled and surface roughness can be determined. Therefore, AFM scans were performed to investigate the molecular arrangement and surface roughness of multilayer polyelectrolyte thin films with different architectures and different surface material components. Images were collected with AFM for fields of 40×40 μm and 5×5 μm for each of the nanofilm samples.

3) Monolayer Cell Culture: To investigate cell behavior on these polyelectrolyte nanofilms, monolayer cell culture methods were applied in the experiments. Cell culture substrates were sterilized in 1× ABAM solution for one hour before transfer to glass-bottom six-well cell culture dishes containing RPMI 1640 complete cell culture medium. RASMCs were seeded into the wells, at approximately 6×10^4 cells/mL with 3 mL of total media volume per well. After cell passage, culture dishes holding substrates with cells were placed in a humidified incubator, and maintained at 37 °C, 5% CO_2 and 95% air. RPMI 1640 complete cell culture media was changed every other day over the course of the culture period. Cell behavior was observed and imaged with the epifluorescence microscope for a period of up to two weeks for each culture system.

4) Staining Cells: Hoechst 33 342 and Alexa Fluor 488 phalloidin were used at different points to stain the cells. For nuclear staining, cells were rinsed with PBS and subsequently treated with a 1 : 1000 Hoechst 33 242 stock solution for 20 min and a 1 : 500 dilution of propidium iodide stock solution for 10 min at 37 °C in the dark. For actin staining, RASMCs were fixed in 4% paraformaldehyde in PBS for 20 min for phalloidin staining following removal of media and a preliminary wash as stated above. Cells were subsequently subjected to a 4-min treatment of Triton-X 100 detergent for permeabilization. Staining was performed by adding a 1 : 40 phalloidin stock solution for 20 min in the dark at 37 °C. After staining procedures, cells were rinsed with PBS, transferred into separate culture dishes, and viewed using the inverted epifluorescence microscope.

5) Imaging and Statistical Analysis: Following staining, 15 fluorescence images of cells were taken randomly along edges and the center of the substrate for each nanofilm sample. The roundness of cells (aka aspect ratio), defined as the ratio of cell width to cell length, was quantified for each cell. The roundness and number of pseudopodia were measured by manual image analysis for the cells cultured on gelatin-, FN, and PSS-coated polyelectrolyte thin films containing different numbers of layers. Average values and standard deviations were calculated in each case, where the number of measurements was equal to the number of cells in each image. Student's t-tests were then used for hypothesis testing to compare cell morphology and draw a statistical conclusion regarding the effect of nanofilms from the experimental data. Pairwise tests were used to determine significance between different numbers of layers and surface coatings.

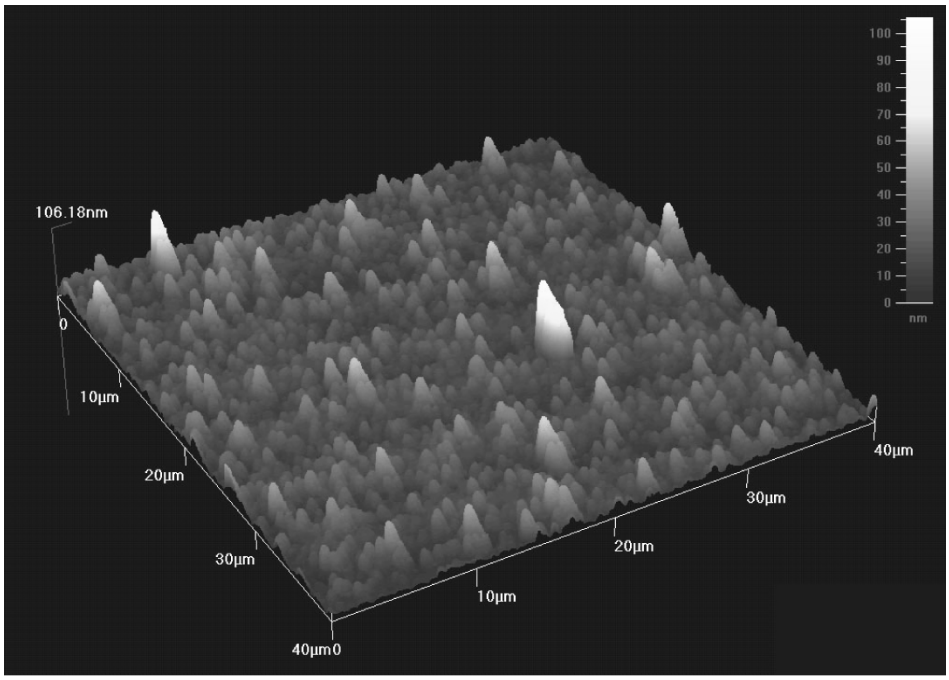

Fig. 3. AFM image of FN-terminated nanofilm $\{(\text{PAH/PSS})_5/\text{FN}\}$ deposited on a glass substrate.

III. Results and Discussion

It was hypothesized that both surface chemistry and roughness would affect the behavior of RASMCs in an *in vitro* cell culture system, as indicated by previous studies [19], [33], [34]. To determine the surface structure of the nanofilms, AFM was used to characterize the surface roughness for samples of varying composition and thickness. AFM measurements were first performed for PSS-coated polyelectrolyte ultrathin films deposited on glass substrates with different underlying bilayers of $(\text{PAH/PSS})_n$, where $n = 2,\ 5,\ 10,$ or 20. Fig. 1 contains a representative AFM image of a 10-bilayer nanofilm with PSS as the terminal layer. The data show that PSS-coated surface is smooth, with an average roughness of 10–20 nm, a value that is comparable to other published data for similar nanofilms [35]. Table I contains the measured roughness values for all PSS-coated substrates. These data also show that the roughness increases with the number of polyelectrolyte layers.

In contrast, it was observed that gelatin molecules did not uniformly cover the entire surface of the nanofilms, as shown in Fig. 2. This explains previous inconsistencies observed in measurements of gelatin adsorption using quartz crystal microbalance (QCM) and zeta-potential measurements [36]. The measurement of average roughness for these surfaces does not reflect the true surface roughness due to the nonuniform coating of gelatin molecules. The gelatin deposited on the PAH-terminated multilayer films appears to form clusters on the surface, and these clusters are not consistent in size, shape, or spacing.

As reported previously, FN can be adsorbed onto a polyelectrolyte nanofilm by incubation in FN solution overnight [35]. An AFM scan of FN-coated PAH/PSS nanofilms (Fig. 3) revealed that, unlike gelatin, FN molecules uniformly cover the entire surface of the polyelectrolyte films. The surface roughness for the PAH/PSS films coated with FN was also measured for each of the samples, and these data are tabulated in Table II. Similar to what was found for PSS/PAH multilayers (Table I), the roughness of FN-coated PSS/PAH surfaces increased with increasing the number of layers

TABLE II
Roughness of FN-Coated (PAH/PSS) Multilayer Nanofilms

# of Bilayers	Nanofilm Architecture	Roughness (nm)	
		Average	S.D.
1	$(\text{PAH/PSS})_1/\text{FN}$	12.24	1.98
2	$(\text{PAH/PSS})_2/\text{FN}$	13.51	2.54
5	$(\text{PAH/PSS})_5/\text{FN}$	16.44	0.70
10	$(\text{PAH/PSS})_{10}/\text{FN}$	23.80	1.54
20	$(\text{PAH/PSS})_{20}/\text{FN}$	28.81	3.80

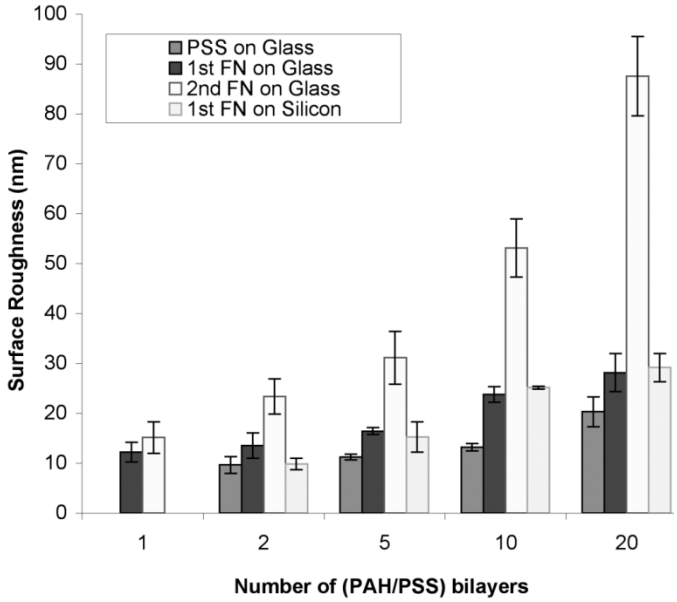

Fig. 4. Comparison of the surface roughness of PSS- and FN-terminated ultrathin films on glass and silicon substrates for different nanofilm thicknesses.

of underlying nanofilms. Compared with the data in Table I, the FN-coated surfaces were around 30% rougher than PSS-coated surface for the same polyelectrolyte architecture.

FN-coated glass substrates were also incubated in FN solution overnight for a second time to further investigate the time-dependent adsorption properties of FN. Fig. 4 is a graph

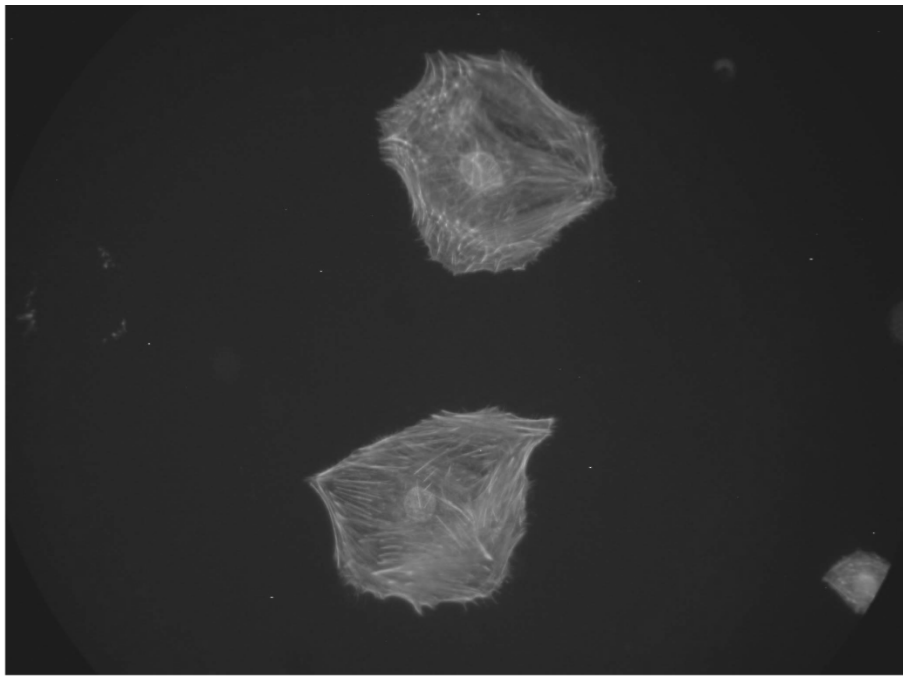

(a)

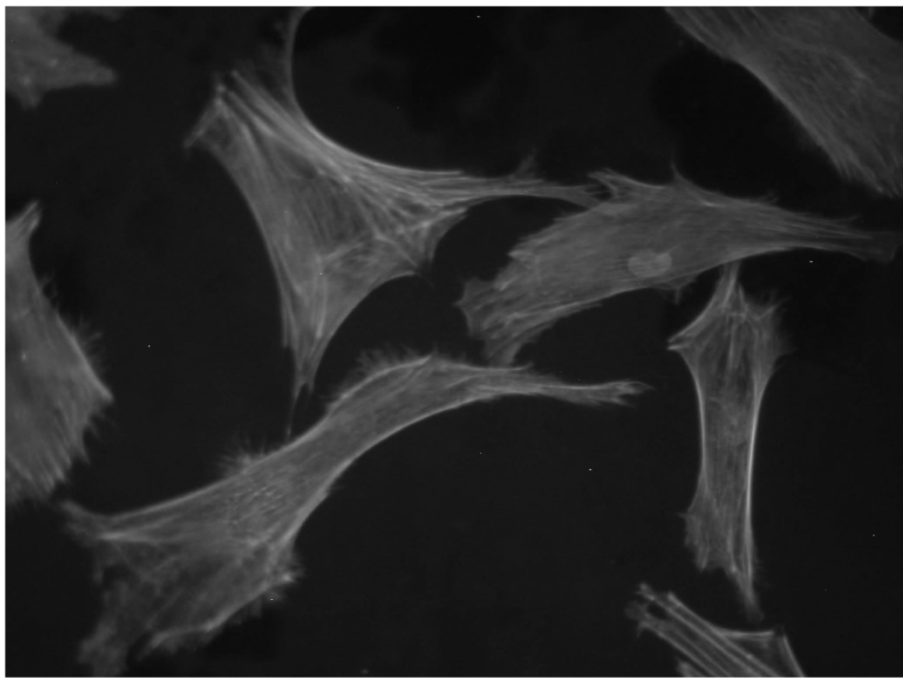

(b)

Fig. 5. Fluorescence images of cells cultured on FN-coated multilayer polyelectrolyte thin films with Hoechst 33 342 and Alexa Fluor 488 phalloidin stain: (a) 1-bilayer; (b) 20-bilayer architecture.

of the roughness of PSS- and FN-coated surfaces with different architectures. The surface roughness of FN-coated nanofilms clearly deviates that measured from PSS-coated surfaces. For both PSS- and FN-coated surfaces, the surface roughness increases as the number of layers of the nanofilms increases. FN-terminated films had consistent roughness properties when deposited on glass and silicon surfaces. Interestingly, the surfaces exposed to FN for a second time show a significant increase in roughness, suggesting additional protein buildup over time due to the presence and contribution of adsorption driving forces other than electrostatics.

Following investigation of adsorption and roughness properties of the different nanofilm structures, the same polyelectrolyte ultrathin films with different PSS, gelatin, and FN surface coatings were used as substrates for cell culture to investigate the relative dependence of cell attachment on surface chemistry, roughness, and underlying nanoarchitecture. Figs. 5–7 contain images of cells cultured on substrates of different surface ma-

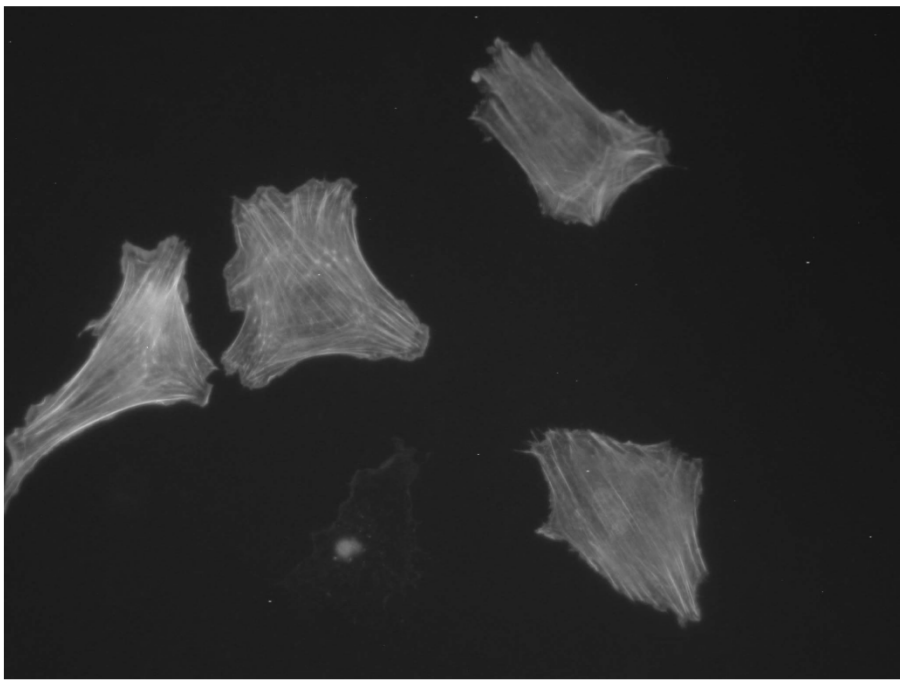

(a)

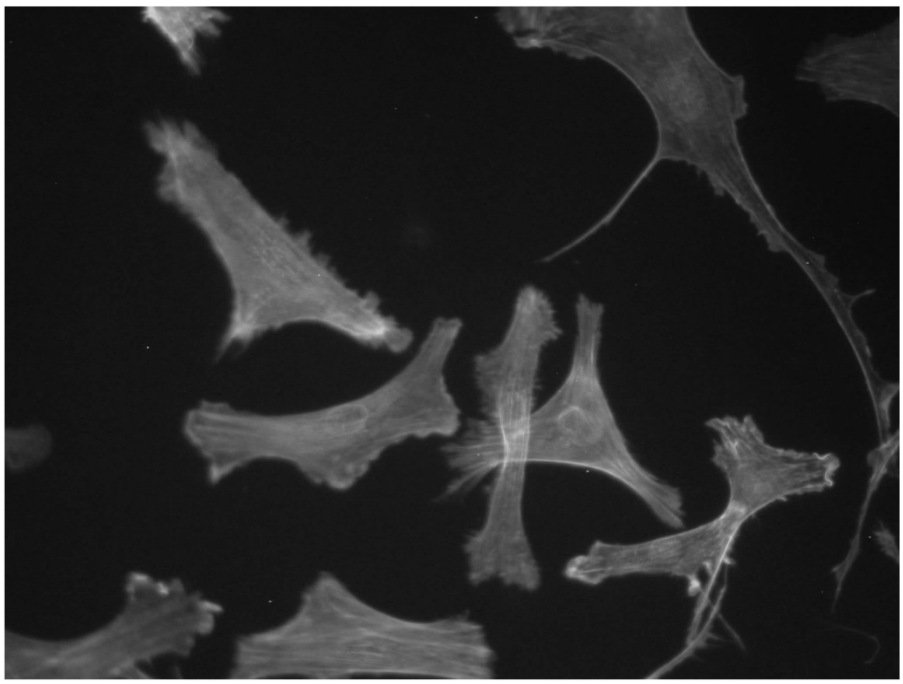

(b)

Fig. 6. Fluorescence images of cells cultured on gelatin-coated multilayer polyelectrolyte thin films with Hoechst 33 342 and Alexa Fluor 488 phalloidin stain: (a) 1-bilayer; (b) 20-bilayer architecture.

terial and thickness and stained with Hoechst 33 342 and Alexa Fluor 488 phalloidin.

Fluorescence images of cells on FN-coated multilayer polyelectrolyte films with architecture of $(\text{PAH/PSS})_n + \text{FN}$, where $n = 1$ and 20, are shown in Fig. 5. From these images, one can qualitatively observe that cells possess a relatively rounded shape when grown on FN-coated 1-bilayer polyelectrolyte thin film surfaces. In contrast, cells have a more spread-out, elongated appearance on FN-coated 20-bilayer films. Furthermore, the cells grown on the thicker films exhibit more pseudopodia than cells grown on thinner nanofilms, suggesting more motile cells. The cell shape and number of pseudopodia were manually determined for a series of images and included in Figs. 8 and 9 to allow comparison of cell properties for different nanofilm susbtrates, as discussed below.

Fig. 6 contains fluorescence images of SMCs cultured on gelatin-coated multilayer polyelectrolyte thin films with layering architecture of $(\text{PAH/PSS})_n + \text{PAH/gelatin}$, where

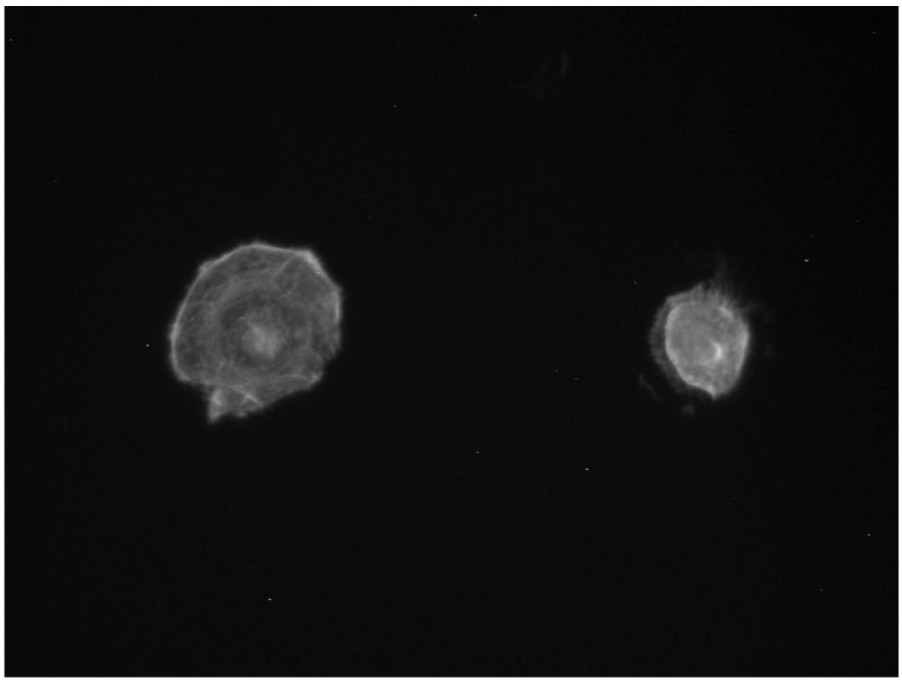

(a)

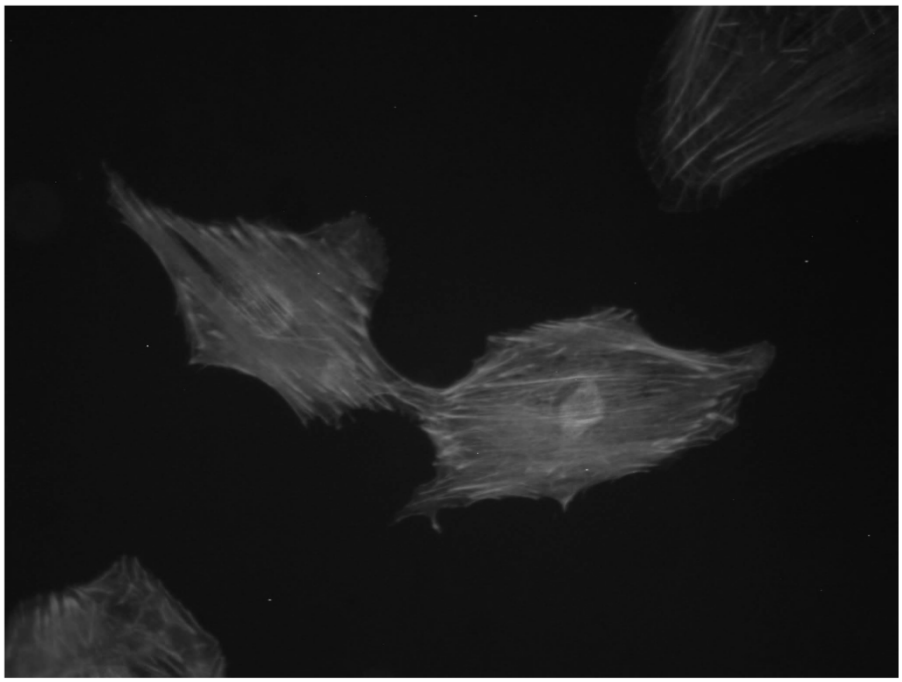

(b)

Fig. 7. Fluorescence images of cells cultured on PSS-coated multilayer polyelectrolyte thin films with Hoechst 33 342 and Alexa Fluor 488 phalloidin stain: (a) 1-bilayer; (b) 20-bilayer architecture.

$n = 1$ and 20. From these images, which are representative of typical observations for the different substrates, it is clear that cells exhibit more elongated and spread-out morphology when grown on 20-bilayer thin films relative to 1-bilayer films, which is similar to the behavior of cells on FN-coated films. In comparing the two cases, it appears that the general characteristics are similar; qualitatively, it appears that the cellular pseudopodia are less sharp on the gelatin-coated films, suggesting relatively lower motility compared to cells on FN-coated surface. However, these observations must be further verified with direct quantitative measurement of cell migration.

Fluorescence images of SMCs cultured on $(\text{PAH/PSS})_n$ multilayer nanofilms ($n = 1$ and 20) are shown in Fig. 7. As is evident from the micrographs, cells displayed more spread morphology on 20-bilayer PSS-coated surfaces than on 1-bilayer PSS surface (similar to what was observed for protein-coated nanofilms). However, the cell morphologies are distinctly different from those seen on FN- and gelatin-coated surfaces when comparing the same number of layers in the

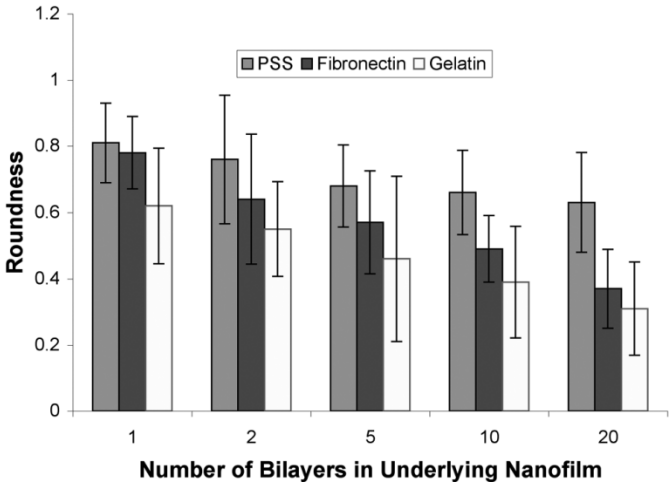

Fig. 8. Roundness of SMCs on PSS-, FN-, and gelatin-coated multilayer polyelectrolyte thin films.

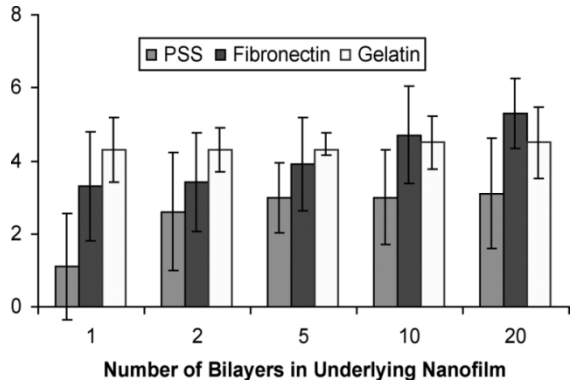

Fig. 9. Number of pseudopodia of SMCs on PSS-, FN-, and gelatin-coated multilayer polyelectrolyte thin films.

underlying polymer nanofilm architecture. Specifically, in Fig. 7(a), cells were small and rounded, obviously not fully spread out; although cells spread out more on the 20-bilayer nanofilms in Fig. 7(b), they still possess a relatively round shape, and exhibit fewer pseudopodia than those observed on 20-bilayer FN- and gelatin-coated thin films.

As is well known, the exposed functional groups on the surface of substrates, such as the RGD amino acid sequence known to be an integrin-binding domain, are the primary factors for cell attachment and movement [24], [37]. However, the results here show that other factors also play essential roles in determining cell behavior. Comparing the images of cells on 1-bilayer and 20-bilayer thin films with FN, gelatin, and PSS surface coatings, it is evident that both FN and gelatin provide better interfaces for the attachment and movement of SMCs than PSS, most likely due to the specific binding properties of the proteins employed. Furthermore, in all cases, 20-bilayer polymer films more strongly promote cell spreading than 1-bilayer film substrates, regardless of the surface coating material.

To further assess the affect of the underlying nanofilms on cell behavior, SMCs were also cultured on 2-bilayer, 5-bilayer, and 10-bilayer polymer films with FN, gelatin, and PSS coatings. In qualitative comparison, little difference was observed in cell morphology when grown on 2-bilayer and 1-bilayer films, and between those on 10-bilayer and 20-bilayer films. Quantitative measurement and statistical analysis (cell morphometrics) were applied to determine whether significant differences in cell morphologies existed for the various substrates. Figs. 8 and 9 are graphs presenting the dependence of cell roundness and number of cell pseudopodia on the number of layers for PSS-, FN-, and gelatin-coated multilayer polyelectrolyte thin films, respectively.

In Fig. 8, the roundness of SMCs on all PSS-, FN-, and gelatin-coated thin films exhibits a general decreasing trend with increasing number of layers in the underlying nanofilms. Student's t-test statistical analysis results, shown in Table III, indicate that there are significant differences between the roundness of cells on 1-bilayer and 20-bilayer polymer thin films for all PSS-, FN-, and gelatin-coated surfaces, which agree with the qualitative analysis above. For FN-coated thin films, there is a significant difference in cell roundness between all 1-, 2-, 5-, 10-, and 20-bilayer thin films, excepting direct comparisons between 2-bilayer to 5-bilayer films, and 5-bilayer to 10-bilayer films. Thus, it appears that the underlying film architectures do play a critical role in resulting cell morphology. For gelatin-coated films, the roundness of cells was observed to decrease gradually with film thickness, and no clear threshold thickness was required to elicit the change. However, for PSS-coated thin films substrates, there were significant changes in cell roundness observed for 1-, 2-, and 10-bilayer films.

In contrast, the number of pseudopodia expressed by cells increased with increasing the number of layers in the underlying architectures for FN-coated thin films. Interestingly, a sharp increase in the number of pseudopodia was observed for PSS-coated films when the underlying architecture increases from 1-bilayer to 2-bilayer, whereas little change takes place between 2-, 5-, 10-, and 20-bilayer films. On the other hand, the number of pseudopodia on gelatin-coated thin films stays essentially constant for all underlying architectures. Compared with cell roundness, statistical analysis results for the number of pseudopodia of cells (Table IV) show similar results to Fig. 9. For PSS-terminated surfaces, it appears that a 2-bilayer film is the threshold architecture for causing cell spreading and increasing the number of pseudopodia. With gelatin-coated nanofilms, no significant difference in the number of pseudopodia was found when comparing films of different underlying architectures. For FN-coated surfaces, the number of cell pseudopodia was found to increase significantly for 10- and 20-bilayer architectures.

Some additional interesting observations were made of cell interactions with the different surfaces. First, an increasing background signal from the staining of the nanofilms was observed with increasing layers of polyelectrolyte thin films. From Fig. 5(b), it can be seen that the 20-bilayer nanofilms emit a brighter blue color, indicating they were stained by Hoechst 33 342, whereas the 1-bilayer nanofilm did not show significant levels of this nonspecific background staining. The likely explanation for this is the ability of the small, cationic Hoechst 33 342 molecules to penetrate the polyelectrolyte films and find negative charges to compensate, as has been demonstrated previously for similar situations [38]. For thicker films, more of these charges are present, leading to stronger background signals. It is possible to control the internal charge properties of the films using varying assembly conditions, allowing a reduction of this background signal if necessary [39]. This may

TABLE III
PROBABILITY OF SIGNIFICANCE IN COMPARISON OF MORPHOLOGY FOR CELLS ON NANOFILMS OF VARYING THICKNESS (PAIRED t-TEST, $n = 15$)

Groups	Roundness of Cells			Number of Pseudopodia		
	PSS	Fibronectin	Gelatin	PSS	Fibronectin	Gelatin
1- Vs. 2-bilayer	0.1956	0.0105*	0.1127	0.0110*	0.4495	0.5000
1- Vs. 5-bilayer	0.0031**	$4x10^{-5}$**	0.0258*	0.0010**	0.1239	0.5000
1- Vs. 10-bilayer	0.0015**	$1x10^{-8}$**	$4x10^{-4}$**	0.0007**	0.0058**	0.2539
1- Vs. 20-bilayer	0.0005**	$6x10^{-11}$**	$4x10^{-6}$**	0.0005**	0.0001**	0.2821
2- Vs. 5-bilayer	0.1028	0.1036	0.1234	0.2126	0.1383	0.5000
2- Vs. 10-bilayer	0.0677*	0.0064**	0.0040**	0.2413	0.0056**	0.2112
2- Vs. 20-bilayer	0.0295*	$4x10^{-5}$**	$3x10^{-5}$**	0.1853	0.0001**	0.2539
5- Vs. 10-bilayer	0.3488	0.0833	0.1708	0.5000	0.0525	0.1912
5- Vs. 20-bilayer	0.1729	0.0004**	0.0225*	0.3901	0.0016**	0.2418
10- Vs. 20-bilayer	0.2867	0.0029**	0.0850	0.4025	0.1098	0.5000

Note: Significance * P<0.05; ** P<0.01.

TABLE IV
PROBABILITY OF SIGNIFICANCE IN COMPARISON OF MORPHOLOGY FOR CELLS ON NANOFILMS WITH DIFFERENT OUTER COATING (PAIRED t-TEST, $n = 5$)

	PSS-Fibronectin	PSS-Gelatin	Fibronectin-Gelatin
Roundness	0.0109*	0.0003**	0.0016**
Number of Pseudopodia	0.0034**	0.0033**	0.2435

Note: Significance * P<0.05; ** P<0.01.

be an important consideration for any studies of cell culture with nanofilms that require staining to assess cell properties.

A second interesting phenomenon was that cells plated onto gelatin-coated thin films needed much less time to attach to the surface than those on FN-coated films. Normally, cells settled and attached on gelatin-coated surfaces in about three hours, then spread out across the culture surface, while it took more than 12 hours for full cell attachment to FN-coated surfaces. Cells plated onto PSS-terminated thin films took much more time to attach on the surface than those on FN- and gelatin-coated films (about one day).

IV. CONCLUSION

Electrostatic LbL self-assembly is a simple and efficient approach to modify the surface chemistries and underlying architectures for nanofilms as *in vitro* cell culture scaffolds. It was found that surface roughness increased with increasing thickness (more layers) of multilayer polyelectrolyte ultrathin films, and the properties of cells grown on these different surfaces were influenced by the thickness and surface chemistry. The roundness and number of pseudopodia of RASMCs varied with the changing surface roughness, exhibiting more natural morphology and spread out pattern on the thicker films. The further suggest that PEMs terminated with cell-adhesive proteins promote the attachment and further growth of SMCs, and that this property is dependent upon the underlying film thickness. These findings are significant in that they demonstrate that modulation of both surface coatings and underlying architecture of nanofilms, both of which may be directly and easily accomplished with the LbL self-assembly, affect the morphology and growth of SMCs. Thus, nanofilm-based scaffolds provide an elegant system for defining the extracellular *in vitro* environment. This work may aid research in tissue and cellular engineering applications, which can benefit from a versatile approach to investigate cell interactions in an *in vitro* environment.

REFERENCES

[1] J. L. Környei, Z. Vértes, K. A. Kovács, P. M. Gócze, and M. Vértes, "Developmental changes in the inhibition of cultured rat uterine cell proliferation by opioid peptides," *Cell Prolif.*, vol. 36, pp. 151–163, 2003.

[2] Y. Li, D. A. Kniss, L. C. Lasky, and S.-T. Yang, "Culturing and differentiation of murine embryonic stem cells in a three-dimensional fibrous matrix," *Cytotechnology*, vol. 41, pp. 23–35, 2003.

[3] E. W. Raines, "The extracellular matrix can regulate vascular cell migration, proliferation, and survival: relationships to vascular disease," *Int. J. Exp. Pathol.*, vol. 81, pp. 173–182, 2000.

[4] M. Lampin, R. Warocquier-Clerout, and M. F. Sigot-Luizard, "Correlation between substratum roughness and wettability, cell adhesion, and cell migration," *J. Biomed. Mater. Res.*, vol. 36, pp. 99–108, 1997.

[5] K. D. Chesmal and J. Black, "Cellular responses to chemical and morphologic aspects of biomaterial surfaces. I. A novel *in vitro* system," *J. Biomed. Mater. Res.*, vol. 29, pp. 1089–1099, 1995.

[6] J. Yang, G. Shi, J. Bei, S. Wang, Y. Cao, Q. Shang, G. Yang, and W. Wang, "Fabrication and surface modification of macroporous poly(L-lactic acid) and poly(L-lactic-co-glycolic acid) (70/30) cell scaffolds for human skin fibroblast cell culture," *J. Biomed. Mater. Res.*, vol. 62, pp. 438–446, 2002.

[7] G. Chen, T. Sato, T. Ushida, N. Ochiai, and T. Tateishi, "Tissue engineering of cartilage using a hybrid scaffold of synthetic polymer and collagen," *Tissue Eng.*, vol. 10, pp. 323–30, 2004.

[8] Y. Zhu, C. Gao, Y. Liu, and J. Shen, "Endothelial cell functions *in vitro* cultured on poly(L-lactic acid) membranes modified with different methods," *J. Biomed. Mater. Res.*, vol. 69A, pp. 436–443, 2004.

[9] Y. Zhu, C. Gao, and J. Shen, "Surface modification of polycaprolactone with poly(methacrylic acid) and gelatin covalent immobilization for promoting its cytocompatibility," *Biomaterials*, vol. 23, no. 7, pp. 4889–4895, 2002.

[10] C. S. Kwok, P. D. Mourad, L. A. Crum, and B. D. Ratner, "Surface modification of polymers with self-assembled molecular structures: multitechnique surface characterization," *Biomacromolecules*, vol. 1, pp. 139–148, 2000.

[11] Y. M. Lvov, K. Ariga, I. Ichinose, and T. Kunitake, "Assembly of multicomponent protein films by means of electrostatic layer-by-layer adsorption," *J. Amer. Chem. Soc.*, vol. 17, pp. 6117–6123, 1995.

[12] Y. M. Lvov, "Electrostatic layer-by-layer assembly of proteins and polyions," in *Protein Architecture: Interfacial Molecular Assembly and Immobilization Biotechnology*, Y. M. Lvov and H. Möwald, Eds. New York: Marcel Dekker, 2000, pp. 125–167.

[13] P. He, N. Hu, and G. Zhou, "Assembly of electroactive layer-by-layer films of hemoglobin and polycationic poly(diallyldimethylammonium)," *Biomacromolecules*, vol. 3, pp. 139–146, 2002.

[14] Y. Wang, W. Du, W. B. Spillman, and R. O. Claus, "Biocompatible thin film coatings frabricated using the electrostatic self-assembly process," in *Proc. SPIE*, vol. 4265, 2001, pp. 142–151.

[15] P. Leclere, A. Calderone, K. Mullen, J. L. Bredas, and R. Lazzaroni, "Conjugated polymer chains self-assembly: a new method to generate (semi)-conducting nanowires," *Mater. Sci. Technol.*, vol. 18, no. 7, pp. 749–754, 2002.
[16] E. Vazques, D. M. Dewitt, P. T. Hammond, and D. M. Lynn, "Construction of hydrolytically-degradable thin films via layer-by-layer deposition of degradable polyelectrolytes," *J. Amer. Chem. Soc.*, vol. 124, pp. 13 992–13 993, 2002.
[17] M. C. Berg, J. Choi, P. T. Hammond, and M. F. Rubner, "Tailored micropatterns through weak polyelectrolyte stamping," in *Langmuir*, 2003, vol. 19, pp. 2231–2237.
[18] Y. Zhu, C. Gao, T. He, X. Liu, and J. Shen, "Layer-by-layer assembly to modify poly(L-lactic acid) surface toward improving its cytocompatibility to human endothelial cells," *Biomacromolecules*, vol. 4, pp. 446–452, 2003.
[19] J. D. Mendelsohn, S. Y. Yang, J. Hiller, A. I. Hochbaum, and M. F. Rubner, "Rational design of cytophilic and cytophobic polyelectrolyte multilayer thin films," *Biomacromolecules*, vol. 4, pp. 96–106, 2003.
[20] P. Tyroen-Tóth, D. Vautier, Y. Haikel, J. Voegel, P. Schaaf, J. Chluba, and J. Ogier, "Viability, adhesion, and bone phenotype of osteoblast-like cells on polyelectrolyte multilayer films," *J. Biomed. Mater. Res.*, vol. 60, pp. 657–667, 2002.
[21] J. T. Elliott, A. Tona, J. T. Woodward, P. L. Jones, and A. L. Plant, "Thin films of collagen affect smooth muscle cell morphology," in *Langmuir*, 2003, vol. 19, pp. 1506–1514.
[22] M. Radhika, M. Babu, and P. K. Sehgal, "Cellular proliferation on desamidated collagen matrices," *Comp. Biochem. Physiol. C. Pharmacol. Toxicol. Endocrinol.*, vol. 124, pp. 131–139, 1999.
[23] R. S. Bhati, D. P. Mukherjee, K. J. McCarthy, S. H. Rogers, D. F. Smith, and S. W. Shalaby, "The growth of chondrocytes into a fibronectin-coated biodegradable scaffold," *J. Biomed. Mater. Res.*, vol. 56, pp. 74–82, 2001.
[24] J. V. Moyano, A. Maqueda, J. P. Albar, and A. Garcia-Pardo, "A synthetic peptide from the heparin-binding domain III (Repeats III4-5) of fibronectin promotes stress-fiber and focal-adhesion formation in melanoma cells," *Biochem. J.*, vol. 371, pp. 565–571, 2003.
[25] A. S. Goldstein and P. A. Dimilla, "Effect of adsorbed fibronectin concentration on cell adhesion and deformation under shear on hydrophobic surfaces," *J. Biomed. Mater. Res.*, vol. 59, pp. 665–675, 2002.
[26] M. Huber, P. Heiduschka, S. Kienle, C. Pavlidis, J. Mack, T. Walk, G. Jung, and S. Thanos, "Modification of glassy carbon surfaces with synthetic laminin-derived peptides for nerve cell attachment and neurocite growth," *J. Biomed. Mater. Res.*, vol. 41, pp. 278–288, 1998.
[27] M. Takagi, K. Shiwaku, T. Inoue, Y. Shirakawa, Y. Sawa, H. Matsuda, and T. Yoshida, "Hydrodynamically stable adhesion of endothelial cells onto a polypropylene hollow fiber membrane by modification with adhesive protein," *J. Artif. Organs.*, vol. 6, no. 3, pp. 222–226, 2003.
[28] J. L. Cuy, B. L. Beckstead, C. D. Brown, A. S. Hoffman, and C. M. Giachelli, "Adhesive protein interactions with chitosan: consequences for valve endothelial cell growth on tissue-engineering materials," *J. Biomed. Mater. Res.*, vol. 67A, pp. 538–547, 2003.
[29] N. Faucheux, R. Schweiss, K. Lutzow, C. Werner, and T. Groth, "Self-assembled monolayers with different terminating groups as model substrates for cell adhesion studies," *Biomaterials*, vol. 25, pp. 2721–2730, 2004.
[30] D. W. Grainger, G. Pavon-Djavid, V. Migonney, and M. Josefowicz, "Assessment of fibronectin conformation adsorbed to polytetrafluoroethylene surfaces from serum protein mixtures and correlation to support of cell attachment in culture," *J. Biomater. Sci. Polym. Ed.*, vol. 14, pp. 973–988, 2003.
[31] M. Li, D. K. Mills, T. Cui, and M. J. McShane, Differential response of smooth muscle cells to polyelectrolyte nanofilms with patterned protein coatings. Manuscript in preparation.
[32] A. P. Ngankam, G. Mao, and P. R. Van Tassel, "Fibronectin adsorption onto polyelectrolyte multilayer films," *Langmuir*, vol. 20, pp. 3362–3370, 2004.
[33] R. L. Price, K. Ellison, K. M. Haberstroh, and T. J. Webster, "Nanometer surface roughness increases select osteoblast adhesion on carbon nanofiber compacts," *J. Biomed. Mater. Res.*, vol. 70A, pp. 129–138, 2004.
[34] A. R. El-Ghannam, P. Ducheyne, M. Risbud, C. S. Adams, I. M. Shapiro, D. Castner, S. Golledge, and R. J. Composto, "Model surfaces engineered with nanoscale roughness and RGD tripeptides promote osteoblast activity," *J. Biomed. Mater. Res.*, vol. 15, pp. 615–627, 2004.
[35] D. S. Salloum and J. B. Schlenoff, "Protein adsorption modalities on polyelectrolyte multilayers," *Biomacromolecules*, vol. 5, pp. 1089–1096, 2004.
[36] M. Li, K. K. Kondabatni, T. Cui, and J. McShane, "Fabrication of 3-D gelatin-patterned glass substrates with layer-by-layer and lift-off (LbL-LO) technology," *IEEE Trans. Nanotechnol.*, vol. 3, no. 1, pp. 115–123, Mar. 2004.
[37] V. Marchi-Artzner, B. Lorz, U. Hellerer, M. Kantlehner, H. Kessler, and E. Sackmann, "Selective adhesion of endothelial cells to artificial membranes with a synthetic RGD-Lipopeptide," *Chem. Eur. J.*, vol. 7, pp. 1095–1101, 2001.
[38] F. Caruso, H. Lichtenfeld, E. Donath, and H. Moehwald, "Investigation of electrostatic interactions in polyelectrolyte multilayer films: binding of anionic fluorescent probes to layers assembled onto colloids," *Macromolecules*, vol. 32, pp. 2317–2328, 1999.
[39] N. Raghavachari, Y. P. Bao, G. Li, X. Xie, and U. R. Muller, "Reduction of autofluorescence on DNA microarrays and slide surfaces by treatment with sodium borohydride," *Anal. Biochem.*, vol. 312, pp. 101–105, 2003.

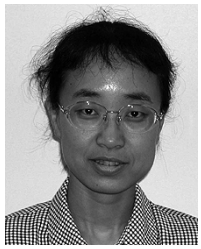

Mengyan Li received the B.S. and M.S. degrees in biomedical engineering from Capital University of Medical Sciences, Beijing, China, in 1995 and 1998, respectively, and the Ph.D. degree in engineering from Louisiana Tech University, Ruston, in 2003.

Currently, she is a Research Postdoctoral Associate in the School of Biomedical Engineering, Science and Health Systems, at Drexel University, Philadelphia, PA. She is working on intelligent three-dimensional scaffolds for tissue engineering in the bionanotechnology area.

David K. Mills received the B.A. degree in history and classics from Indiana University, Bloomington, in 1977, the M.A. degree in anthropology from the University of Illinois, Chicago, in 1983, and the Ph.D. degree in anatomy and cell biology from the University of Illinois at Chicago Medical Center in 1991.

He is an associate professor of biological sciences and the Institute for Micromanufacturing at Louisiana Tech University. His primary research interest is the application of micro- and nanoscale technologies emphasizing cell biology applications.

Tianhong Cui received the B.S. degree from Nanjing University of Aeronautics and Astronautics in 1991 and the Ph.D. degree from the Chinese Academy of Sciences in 1995.

He served as a Postdoctoral Research Associate at the University of Minnesota and Tsinghua University. He was with the National Laboratory of Metrology in Japan as a Research Fellow. He is currently serving as an Assistant Professor of Electrical Engineering, Institute for Micromanufacturing, Louisiana Tech University, Ruston. His current research interests include microelectromechanical systems (MEMS), nanotechnology, and polymer micro/nanoelectronics.

Michael J. McShane (S'96, M'00) received the B.S. degree in bioengineering and the Ph.D. degree in biomedical engineering from Texas A&M University, College Station, in 1994 and 1999, respectively.

He is an Associate Professor of Biomedical Engineering at Louisiana Tech University, Ruston, and a Research Associate of the university's Institute for Micromanufacturing (IfM). His primary research interests are the development of novel instrumentation for physical and chemical biomedical measurements, particularly optical sensors, and applications of micro/nanoengineering to medicine and biology. A major emphasis area for his research is implantable microsphere sensors ("smart tattoos") for metabolic monitoring, especially noninvasive glucose sensing.